PHYSICAL REVIEW D **85,** 074026 (2012)

# Prompt heavy quarkonium production in association with a massive (anti)bottom quark at the LHC

Li Gang, Wang ShuangTe, Song Mao, and Lin JiPing

*School of Physics Material Science, Anhui University, Hefei, Anhui 230039, P.R. China*

(Received 28 November 2011; published 24 April 2012)

In this work, we investigate the associated production of prompt heavy quarkonium and a massive (anti) bottom quark to leading order in the nonrelativistic QCD factorization formalism at the LHC. We present numerical results for the processes involving $J/\psi$, $\chi_{cJ}$, $\Upsilon$ and $\chi_{bJ}$. From our work, we find that the production rates of these processes are quite large, and these processes have the potential to be detected at the LHC. When $p_T$ is smaller than about 10 GeV, the $c\bar{c}[^1S_0^{(8)}]$ states give the main contribution to the $p_T$ distribution of prompt $J/\psi$ with a massive (anti)bottom quark production. For the process $pp \to \Upsilon + b(\bar{b})$, the contribution of the color-singlet mechanism is larger than that in the color-octet mechanism at low $p_T$ region. We also investigate the processes $pp \to \chi_{cJ} + b(\bar{b})$ and $pp \to \chi_{bJ} + b(\bar{b})$; the $p_T$ distributions are dominated by the color-octet Fock-state contribution at large $p_T$. These processes provide an interesting signature that could be studied at the LHC, and the measurement of these processes is useful to test the color-singlet mechanism and color-octet mechanism.

DOI: 10.1103/PhysRevD.85.074026 PACS numbers: 12.38.Bx, 13.60.Le, 13.85.Ni, 14.40.Pq

## I. INTRODUCTION

A heavy quarkonium is made of a heavy quark and a heavy antiquark; its decay and production can be factorized into a short-distance part, which can be calculated in QCD perturbatively, and a long-distance part, which is governed by nonperturbative QCD dynamics. So the study of heavy quarkonium offers a good testing ground for investigating the strong interaction in both perturbative and nonperturbative level in high-energy physics.

In the early days, based on the factorization formalism, color-singlet mechanism (CSM) [1] was used to describe the production and decay of heavy quarkonium, and obtained some phenomenological successes. However, the CSM has encountered many difficulties in various theoretical [2] and experimental aspects [3], such as the appearance of a logarithmic infrared divergence in the case of next-to-leading-order (NLO) $P$-wave decays into light hadrons and the huge discrepancy of the high-$p_T$ $J/\psi$ production between the theoretical prediction and the experimental measurement at the Tevatron. To solve these formal and phenomenological problems of CSM, a rigorous theory, nonrelativistic QCD (NRQCD) [4] was proposed by Bodwin, Braaten and Lepage (BBL). In the NRQCD, the idea of perturbative factorization is retained, the processes of production and decay of heavy quarkonium are also separated into two parts: a short-distance part and long-distance matrix elements (LDMEs), which can be extracted from experiments. The relative importance of the LDMEs can be estimated by means of the velocity-scaling rules [5].

The vital difference between NRQCD and the traditional color-singlet model is that, in NRQCD, the complete structure of the quarkonium Fock space has been explicitly considered, and NRQCD predicts the existence of color-octet (CO) processes in nature. This CO theory allows that $Q\bar{Q}$ pairs can be produced at short distance in CO states and subsequently evolved into physical, color-singlet (CS) quarkonium through emission of soft gluons at nonperturbative process [6]. Being introduced to the color-octet mechanism (COM), NRQCD has absorbed the infrared divergences in P-wave [4,7,8] and D-wave [9,10] decay widths of heavy quarkonium and successfully reconciled the orders of magnitude discrepancy between the experimental data of $J/\psi$ production at the Tevatron [11] and the leading-order (LO) CSM theoretical predictions at large $p_T$.

Recently, in order to clarify the validity and limitation of the NRQCD formalism, substantial progress has been achieved in the calculations of heavy quarkonium production. The DELPHI data favor the NRQCD COM prediction for the $\gamma\gamma \to J/\psi + X$ process [12]. Similarly, the recent experimental data on the $J/\psi$ photoproduction of H1 [13] are fairly well-described by the complete NLO NRQCD corrections [14], which give strong support to the existence of the COM. However, at B factories, a series of processes were calculated up to the QCD NLO corrections in the CSM [15–17]. Together with the relativistic correction [18,19], it seems that most experimental data could be understood. Additionally, the $J/\psi$ polarization in hadroproduction at the Tevatron [20] and photoproduction at the HERA [21] also conflict with the NRQCD predictions. So the existence of the COM is still under question and far from being proven. Therefore, the further test for the CSM and COM under NRQCD in heavy quarkonium production is still needed.

In order to investigate the effects of the CSM and COM in heavy quarkonium physics, more processes of heavy quarkonium production and decay should be studied. At the LHC, with more attention for the heavy quarkonium

 

production, much work has been done in these regions [22,23], and some channels have been calculated to the NLO [24–26]. As quarkonium can be identified by using their purely leptonic decays [27,28], the bottom quark can be identified by reconstructing secondary vertices, and the high-$p_T$ bottom quark can be tagged with reasonably high efficiency at the LHC, meanwhile the observation of a bottom quark with high-$p_T$ can reduce the backgrounds of the heavy quarkonium production. Thus, it is also very interesting to study the prompt heavy quarkonium production associated with a massive (anti)bottom quark at the LHC. These processes have the potential to be detected and can provide an interesting signature at the LHC. The measurement of these processes is useful to test the CSM and COM.

In this work, we perform the calculations for prompt heavy quarkonium production in association with a massive (anti)bottom quark at the LHC. Within this work, the mass of bottom quark is retained in all the partonic processes. The paper is organized as follows: We present the details of the calculation strategies in Sec. II. The numerical results are given in Sec. III. Finally, a short summary and discussions are given.

## II. THE DETAILS OF THE CALCULATION

The purpose of this paper is to study the associated production of prompt heavy quarkonium and a massive (anti)bottom quark to LO in the NRQCD factorization formalism at the LHC. We denote the heavy quarkonium as $\mathcal{Q}$. As we know, the cross section for the $g(p_1) + b(p_2) \to \mathcal{Q}(k_3) + b(k_4)$ partonic process in the SM should be the same as that for its charge conjugate subprocess $g(p_1) + \bar{b}(p_2) \to \mathcal{Q}(k_3) + \bar{b}(k_4)$, and the luminosity of the bottom quark in a proton is same as that of the antibottom quark. Therefore, the production rates of the $\mathcal{Q}b$ and the $\mathcal{Q}\bar{b}$ are identical at the LHC. In the following sections, we present only the analytical calculations of the related partonic process $g(p_1) + b(p_2) \to \mathcal{Q}(k_3) + b(k_4)$ and the parent process $pp \to \mathcal{Q} + b$ unless otherwise indicated.

The cross section for the $pp \to \mathcal{Q} + b$ process is expressed as

$$\sigma(pp \to \mathcal{Q} + b) = \int dx_1 dx_2 \sum_n \langle \mathcal{O}^{\mathcal{Q}}[n] \rangle \hat{\sigma}(gb \to Q\bar{Q}[n] + b) \times [G_{g/A}(x_1, \mu_f) G_{b/B}(x_2, \mu_f) + (A \leftrightarrow B)]. \quad (1)$$

Here $\hat{\sigma}(gb \to Q\bar{Q}[n] + b)$ describes the short-distance production of a heavy $Q\bar{Q}$ pair in the color, spin, and angular momentum state $n$. When $Q = c$, $\mathcal{Q}$ represents charmonium and when $Q = b$, $\mathcal{Q}$ is bottomonium. $\langle \mathcal{O}^{\mathcal{Q}}[n] \rangle$ is the long-distance matrix element, which describes the hadronization of the heavy $Q\bar{Q}$ pair into the observable quarkonium state $\mathcal{Q}$. $G_{b,g/A,B}$ are the parton distribution functions. $A$ and $B$ refer to protons at the LHC. The indices $g$, $b$ represents the gluon and bottom quark, respectively.

The short-distance cross section for the production of a $Q\bar{Q}$ pair in a Fock state $n$, $\hat{\sigma}[gb \to Q\bar{Q}[n] + b]$, is calculated from the amplitudes which are obtained by applying certain projectors onto the usual QCD amplitudes for open $Q\bar{Q}$ production. In the notations of Ref. [8]:

$$\begin{aligned} \mathcal{A}_{Q\bar{Q}[^1S_0^{(1/8)}]} &= \mathrm{Tr}[\mathcal{C}_{1/8} \Pi_0 \mathcal{A}]_{q=0}, \\ \mathcal{A}_{Q\bar{Q}[^3S_1^{(1/8)}]} &= \mathcal{E}_\alpha \mathrm{Tr}[\mathcal{C}_{1/8} \Pi_1^\alpha \mathcal{A}]_{q=0}, \\ \mathcal{A}_{Q\bar{Q}[^1P_1^{(1/8)}]} &= \mathcal{E}_\alpha \frac{d}{dq_\alpha} \mathrm{Tr}[\mathcal{C}_{1/8} \Pi_0 \mathcal{A}]_{q=0}, \\ \mathcal{A}_{Q\bar{Q}[^3P_J^{(1/8)}]} &= \mathcal{E}^{(J)}_{\alpha\beta} \frac{d}{dq_\beta} \mathrm{Tr}[\mathcal{C}_{(1/8)} \Pi_1^\alpha \mathcal{A}]_{q=0}, \end{aligned} \quad (2)$$

where $\mathcal{A}$ denotes the QCD amplitude with amputated heavy-quark spinors, the lower index $q$ represents the momentum of the heavy-quark in the $Q\bar{Q}$ rest frame. $\Pi_{0/1}$ are spin projectors onto the spin singlet and spin triplet states. $\mathcal{C}_{1/8}$ are color projectors onto the color-singlet and color-octet states. $\mathcal{E}_\alpha$ and $\mathcal{E}_{\alpha\beta}$ represent the polarization vector and tensor of the $Q\bar{Q}$ states, respectively.

Then the LO short-distance cross section for the partonic process $g(p_1) + b(p_2) \to Q\bar{Q}[n](k_3) + b(k_4)$ is obtained by using the following formula:

$$\hat{\sigma}(gb \to Q\bar{Q}[n] + b) = \frac{1}{16\pi \hat{s}^2 N_{col} N_{pol}} \int_{\hat{t}_{\min}}^{\hat{t}_{\max}} d\hat{t} \sum |\mathcal{A}_{Q\bar{Q}[n]}|^2. \quad (3)$$

The summation is taken over the spins and colors of initial and final states, and the bar over the summation denotes averaging over the spins and colors of initial partons. The Mandelstam variables are defined as: $\hat{s} = (p_1 + p_2)^2$, $\hat{t} = (p_1 - k_3)^2$, $\hat{u} = (p_1 - k_4)^2$. $N_{col}$ and $N_{pol}$ refer to the numbers of colors and polarization of states $n$, separately [8]. In this paper, we present all contributing partonic cross sections in analytic form in the Appendix.

In the case of prompt charmonium production in association with a massive bottom quark, there are five Feynman diagrams that contribute to this process at LO; we present them in Fig. 1. There are 10 Feynman diagrams for prompt bottomonium partonic process, which are drawn in Fig. 2. In our calculations, the $Q\bar{Q}$ Fock states contributing at LO in $v$ for $\mathcal{Q}$ are shown in Table I.

Following the heavy-quark spin symmetry, these multiplicity relations of LDMEs

$$\begin{aligned} \langle \mathcal{O}^{\psi(nS)}[^3P_J^{(8)}] \rangle &= (2J+1) \langle \mathcal{O}^{\psi(nS)}[^3P_0^{(8)}] \rangle, \\ \langle \mathcal{O}^{\Upsilon(nS)}[^3P_J^{(8)}] \rangle &= (2J+1) \langle \mathcal{O}^{\Upsilon(nS)}[^3P_0^{(8)}] \rangle, \\ \langle \mathcal{O}^{\chi_{QJ}}[^3P_J^{(1)}] \rangle &= (2J+1) \langle \mathcal{O}^{\chi_{Q0}}[^3P_0^{(1)}] \rangle, \\ \langle \mathcal{O}^{\chi_{QJ}}[^3S_1^{(8)}] \rangle &= (2J+1) \langle \mathcal{O}^{\chi_{Q0}}[^3S_1^{(8)}] \rangle \end{aligned} \quad (4)$$

are assumed to be satisfied [4].

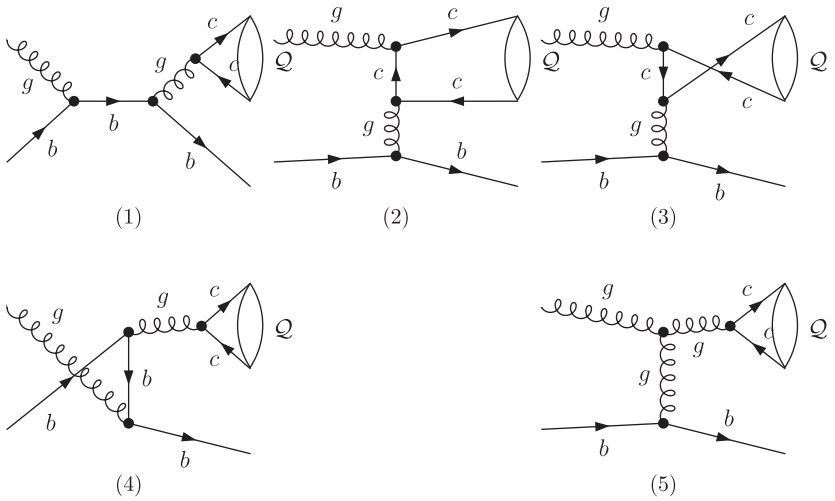


FIG. 1. The LO Feynman diagrams for prompt charmonium production in association with a massive bottom quark at the LHC.

## III. NUMERICAL RESULTS

In our numerical calculations, we focus on the cases $\mathcal{Q} = J/\psi$, $\chi_{cJ}$, $\Upsilon$, $\chi_{bJ}$. These quarkoniums can be efficiently identified experimentally, and their LDMEs are relatively well-constrained [29–33]. The $\eta_c$, $\eta_b$, $h_c$, and $h_b$ mesons are more difficult to detect experimentally, and we will give the differential cross sections relevant to these quarkoniums analytically in our Appendix.

We take CTEQ6L1 parton distribution functions [34] with a one-loop running $\alpha_s$ in the LO calculations, and the corresponding fitted value $\alpha_s(M_Z) = 0.130$ is used for our calculations. The factorization scale is chosen as $\mu_f = m_T$, where $m_T = \sqrt{(p_T^{\mathcal{Q}})^2 + m_{\mathcal{Q}}^2}$ is the $\mathcal{Q}$ transverse mass. The masses of the heavy quark are set as $m_c = 1.5$ GeV and $m_b = 4.75$ GeV.

For CO LDME of $J/\psi$, it can be extracted from experimental data or from lattice QCD calculations. Before lattice QCD giving out the results, the color-octet matrix elements are determined only by fitting the theoretical prediction to experimental data. As done in the literature [19,30], the color-octet matrix elements are extracted from experimental data of $J/\psi$ production in $e^+e^-$, $ep$ collisions and hadron collisions. In Ref. [19], through the analysis of the process $e^+e^- \to J/\psi + X_{\text{non-}c\bar{c}}$ at B factories, they give a very stringent constraint on the CO contribution, and imply that the values of color-octet matrix elements are very small, but their results may not be consistent with the naive velocity-scaling rules. Recently, M. Butenschoen and B. A. Kniehl performed a multiprocess fit of the CO LDMEs [30], givng more global fit results, and their results are consistent with NRQCD scaling rules.

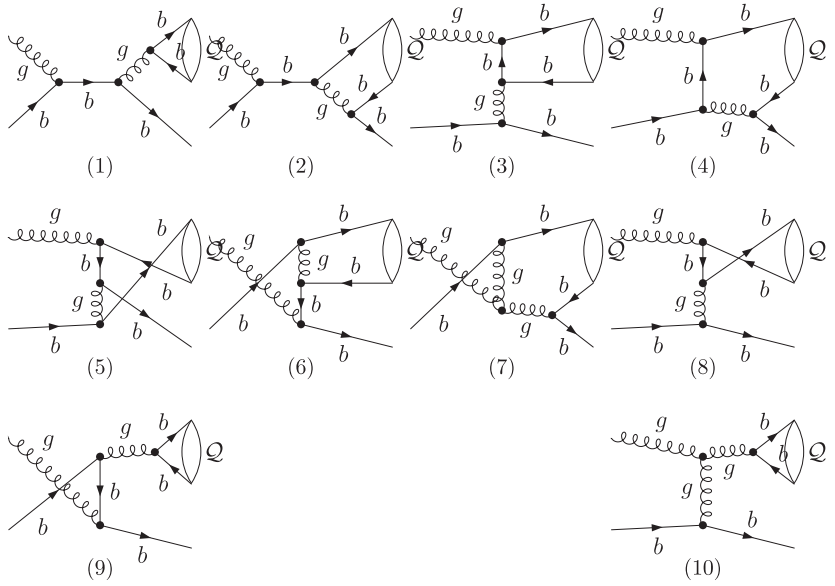


FIG. 2. The LO Feynman diagrams for prompt bottomonium production in association with a massive bottom quark at the LHC.

TABLE I. Values of $k$ in the velocity-scaling rule $\langle \mathcal{O}^{\mathcal{Q}}[n] \rangle \propto v^k$ for the leading $Q\bar{Q}$ Fock states $n$ pertinent to $\mathcal{Q}$.

| k | $\eta_c$, $\eta_b$ | $J/\Psi$, $\Psi'$, $\Psi(3s)\ldots$ $\Upsilon$, $\Upsilon(2s)$, $\Upsilon(3s)\ldots$ | $h_c$, $h_b$ | $\chi_{cJ}$, $\chi_{bJ}$ |
|---|---|---|---|---|
| 3 | $^1S_0^{(1)}$ | $^3S_1^{(1)}$ | - | - |
| 5 | - | - | $^1P_1^{(1)}$, $^1S_0^{(8)}$ | $^3P_J^{(1)}$, $^3S_1^{(8)}$ |
| 7 | $^1S_0^{(8)}$, $^3S_1^{(8)}$, $^1P_1^{(8)}$ | $^1S_0^{(8)}$, $^3S_1^{(8)}$, $^3P_J^{(8)}$ | - | - |

In our work, though we performed a LO calculation, we will tentatively choose the color-octet matrix elements obtained by the M. Butenschoen and B. A. Kniehl's NLO fit results [30]

$$\begin{aligned}\langle O^{J/\psi}[^1S_0^{(8)}]\rangle &= (4.76 \pm 0.71) \times 10^{-2}\ \mathrm{GeV}^3,\\ \langle O^{J/\psi}[^3S_1^{(8)}]\rangle &= (0.265 \pm 0.91) \times 10^{-2}\ \mathrm{GeV}^3,\\ \langle O^{J/\psi}[^3P_0^{(8)}]\rangle &= (-1.32 \pm 0.35) \times 10^{-2}\ \mathrm{GeV}^5,\end{aligned} \tag{5}$$

as our input parameters. The relation of the CS matrix elements $\langle O^{\chi_{c0}}[^3P_0^{(1)}]\rangle$ of $\chi_{c0}$ with the P-wave function at the origin is the formula $\langle O^{\chi_{c0}}[^3P_0^{(1)}]\rangle = \frac{3N_c}{2\pi}|R'_P(0)|^2$, and we choose $|R'_P(0)|^2 = 0.075\ \mathrm{GeV}^5$, from the potential model calculations [31]. For the CO matrix element $\langle O^{\chi_{c0}}[^3S_1^{(8)}]\rangle$, we use $\langle O^{\chi_{c0}}[^3S_1^{(8)}]\rangle \approx 2.2 \times 10^{-3}\ \mathrm{GeV}^3$ as our input parameter [29]. For the NRQCD matrix elements of bottomonium, the CS matrix elements are taken from the potential model calculations of [32], and the CO matrix elements are determined from the CDF data [33]. In our calculations, the relation of CS matrix elements with the conventions matrix elements of Bodwin-Braaten-Lepage is always considered carefully [8].

In our numerical calculations, we summed the contributions of $pp \to \mathcal{Q} + b$ and $pp \to \mathcal{Q} + \bar{b}$. If $\mathcal{Q} = \chi_{QJ}$, we also summed the contributions of $\chi_{Q0}$, $\chi_{Q1}$ and $\chi_{Q2}$. We take the constraints of $|y^{\mathcal{Q}}| < 3$ for heavy quarkoniums, and $p_{T,b(\bar{b})} > 5$ GeV, $|y_{b(\bar{b})}| < 3$ for $b(\bar{b})$ quark. The colliding energy used in this paper is 14 TeV.

In Fig. 3, we present the LO distributions of $p_T^{J/\psi}$ and $y^{J/\psi}$ for the process $pp \to J/\psi + b(\bar{b})$ at the LHC. At LO, the associated production of prompt $J/\psi$ with a (anti) bottom quark is forbidden in the CSM, and there is only CO contribution in this process up to the $\alpha_s^3 v^7$ order within the NRQCD framework. For comparison, we also depicted the contributions of the $c\bar{c}[^1S_0^{(8)}]$, $c\bar{c}[^3S_1^{(8)}]$, and $c\bar{c}[^3P_J^{(8)}]$ Fock states in these figures. For the LDME of $c\bar{c}[^3P_J^{(8)}]$ ($J = 0, 1, 2$), Fock states are negative, the contribution of these Fock states are negative too. In Fig. 3, we present the $p_T$ distributions $-d\sigma/dp_T^{J/\psi}[c\bar{c}[^3P_J^{(8)}]]$ in the $p_T$ distribution figure. From the figure we can see that when $p_T$ is smaller than about 10 GeV, the $1S_0^{(8)}$ state gives the main contribution to the $p_T$ distribution of prompt $J/\psi$ with a (anti)bottom quark production. With the $p_T$ of $J/\psi$ increase, the contributions of $c\bar{c}[^1S_0^{(8)}]$ and $c\bar{c}[^3P_J^{(8)}]$ Fock states quickly decrease. The differential cross section is dominated by the $c\bar{c}[^3S_1^{(8)}]$ Fock-state contribution at large $p_T$ region. In the range of 5 GeV $< p_T^{J/\psi} <$ 50 GeV, the $d\sigma/dp_T^{J/\psi}$ is in the range of [0.486, 3276.396] pb/GeV, and it reaches the maximum when $p_T^{J/\psi} = 5$ GeV.

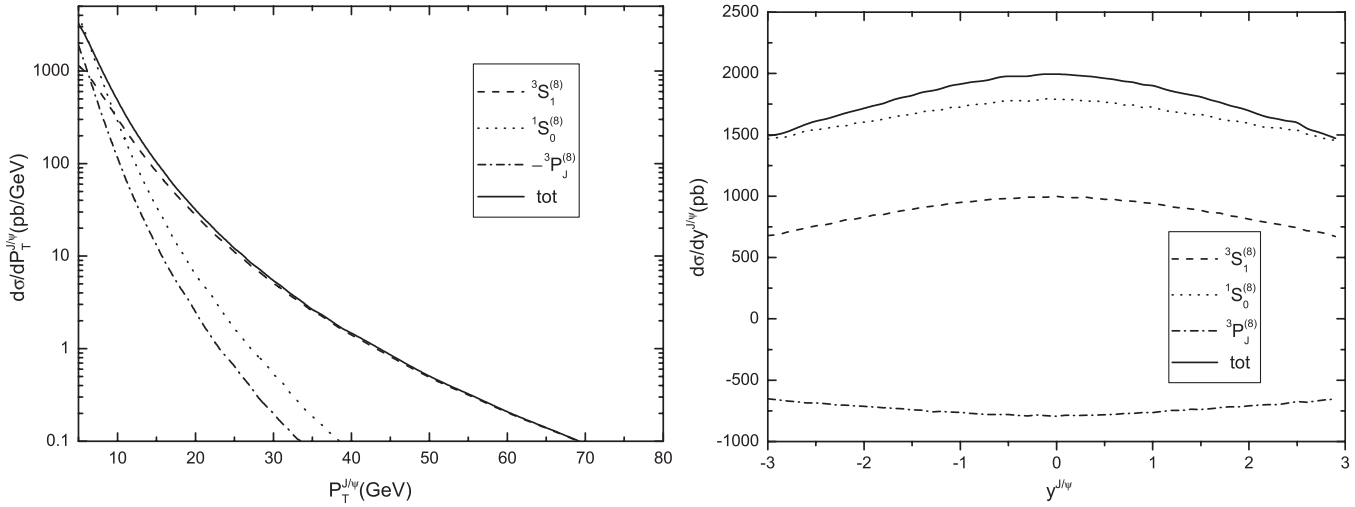


FIG. 3. The LO distributions of $p_T^{J/\psi}$ and $y^{J/\psi}$ for the $pp \to J/\psi + b(\bar{b})$ process, and the contributions of the $c\bar{c}[^1S_0^{(8)}]$, $c\bar{c}[^3S_1^{(8)}]$ and $c\bar{c}[^3P_J^{(8)}]$ Fock states at the LHC.

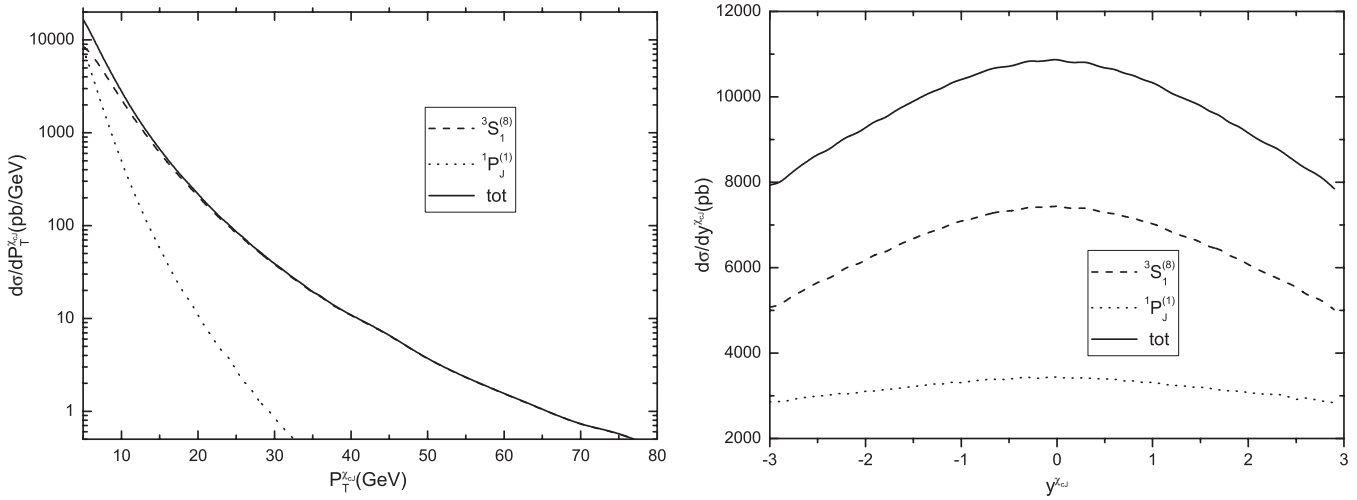


FIG. 4. The LO distributions of $p_T^{\chi_{cJ}}$ and $y^{\chi_{cJ}}$ for the $pp \to \chi_{cJ} + b(\bar{b})$ process, and the contributions of the $c\bar{c}[^3S_1^{(8)}]$ and $c\bar{c}[^3P_J^{(1)}]$ Fock states at the LHC.

The curves for the LO distributions of $p_T^{\chi_{cJ}}$ and $y^{\chi_{cJ}}$ for the process $pp \to \chi_{cJ} + b(\bar{b})$ at the LHC are drawn in Fig. 4. From the figure, we can see that the contribution from CS is about the same order of magnitude with CO at $p_T \simeq 5$ GeV. The CO contribution dominates over production at the large $p_T$ region, and it decreases much more slowly than that of CS as $p_T$ increases. From Fig. 3 and 4, we can find that the cross section of $J/\psi + b(\bar{b})$ and $\chi_{cJ} + b(\bar{b})$ associated production mainly comes from the $c\bar{c}[^3S_1^{(8)}]$ Fock state contribution at large $p_T$ region. The cross section ratios of $J/\psi + b(\bar{b})$ and $\chi_{cJ} + b(\bar{b})$ associated production can be estimated approximately by $\langle \mathcal{O}^{J/\psi}[^3S_1^{(8)}]\rangle / \sum_{J=0}^{2}\langle \mathcal{O}^{\chi_{cJ}}[^3S_1^{(8)}]\rangle \approx 0.134$ at large $p_T$ region [29,30]. So when we consider the process prompt $J/\psi$ with a (anti)bottom quark associated production at the LHC, the indirect prompt production for this process via radiative decays of $\chi_{cJ}$ should be included.

The LO distributions of $p_T^{\Upsilon}$ and $y^{\Upsilon}$ for the process $pp \to \Upsilon + b(\bar{b})$, and the contributions of the $b\bar{b}[^3S_1^{(1)}]$, $b\bar{b}[^1S_0^{(8)}]$, $b\bar{b}[^3S_1^{(8)}]$ and $b\bar{b}[^3P_J^{(8)}]$ Fock states at the LHC are illustrated in Fig. 5. We can see that the differential cross section of $b\bar{b}[^3S_1^{(1)}]$ and $b\bar{b}[^3S_1^{(8)}]$ Fock states give the main contribution to the distributions of $p_T^{\Upsilon}$ for the process $pp \to \Upsilon + b(\bar{b})$ at the LO. The $b\bar{b}[^3S_1^{(1)}]$ state give the main contribution to the $p_T$ distribution at low $p_T$ region. With the increase of $p_T^{\Upsilon}$, the contribution of $b\bar{b}[^3S_1^{(1)}]$ Fock state quickly decreases and the contribution of $b\bar{b}[^3S_1^{(8)}]$ Fock state becomes more important. The contribution of $b\bar{b}[^3S_1^{(8)}]$ Fock states starts to be comparable to $b\bar{b}[^3S_1^{(1)}]$ contribution for $p_T \simeq 22$ GeV. The differential cross section is dominated by the $b\bar{b}[^3S_1^{(8)}]$ Fock state contribution at large $p_T$ region.

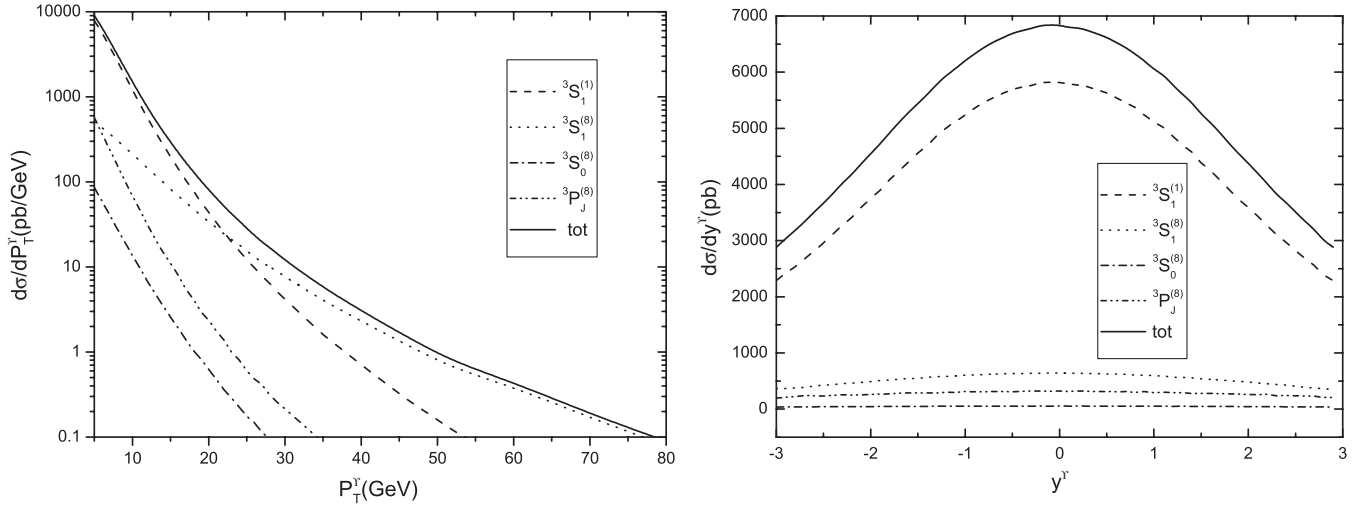


FIG. 5. The LO distributions of $p_T^{\Upsilon}$ and $y^{\Upsilon}$ for the process $pp \to \Upsilon + b(\bar{b})$, and the contributions of the $b\bar{b}[^3S_1^{(1)}]$, $b\bar{b}[^1S_0^{(8)}]$, $b\bar{b}[^3S_1^{(8)}]$ and $b\bar{b}[^3P_J^{(8)}]$ Fock states at the LHC.

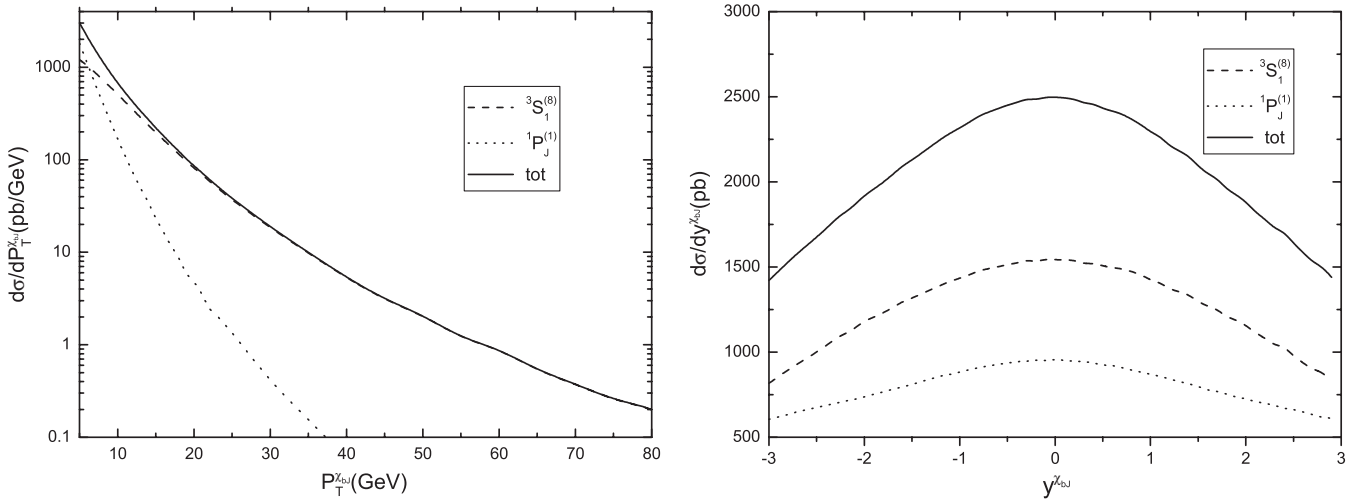


FIG. 6. The LO distributions of $p_T^{\chi_{bJ}}$ and $y^{\chi_{bJ}}$ for the $pp \to \chi_{bJ} + b(\bar{b})$ process, and the contributions of the $b\bar{b}[^3S_1^{(8)}]$ and $b\bar{b}[^3P_J^{(1)}]$ Fock states at the LHC.

In this paper, we have only considered the LO process $pp \to \Upsilon + b(\bar{b}) + X$ at $\alpha_s^3$. In Ref. [23], the authors have evaluated the color-singlet contribution to the process $pp \to \Upsilon + b\bar{b}$. One of the properties of $pp \to \Upsilon + b\bar{b}$ is that its CS contribution (which is at $\alpha_s^4$) already includes $p_T^{-4}$ topologies which dominate at large $p_T$. If we consider the process $pp \to \Upsilon + b(\bar{b}) + X$ at $\alpha_s^4$, the process $pp \to \Upsilon + b\bar{b}$ may give important CS contribution in large $p_T$ region.

Finally, we give the LO distributions of $p_T^{\chi_{bJ}}$ and $y^{\chi_{bJ}}$ for the process $pp \to \chi_{bJ} + b(\bar{b})$, and the contributions of the $b\bar{b}[^3S_1^{(8)}]$ and $b\bar{b}[^3P_J^{(1)}]$ Fock states at the LHC in Fig. 6. From these figures we can see that the contribution from CS is larger than CO when $p_T < 6$ GeV. The CO contribution dominates over production at the large $p_T$ region, and it decreases much slower than that of CS as $p_T$ increases. In the range of 5 GeV $< p_T^{\chi_{bJ}} <$ 50 GeV, the $d\sigma/dp_T^{\chi_{bJ}}$ is in the range of $[2.095, 3022.305]$ pb/GeV, and it reaches the maximum when $p_T^{J/\psi} = 5$ GeV.

## IV. DISCUSSION AND SUMMARY

In this paper, we investigate the associated production of prompt heavy quarkonium with a massive (anti)bottom quark to LO in the NRQCD factorization formalism at the LHC. We have considered all experimentally established heavy quarkoniums, with $^{2S+1}L_J = {}^1S_0$, ${}^3S_1$, ${}^1P_1$, ${}^3P_J$, and listed the differential cross sections relevant to these quarkonium analytically in our Appendix. We present the numerical predictions of the differential cross sections of the $p_T^{\mathcal{Q}}$ and rapidity $y^{\mathcal{Q}}$ for $\mathcal{Q} = J/\psi$, $\chi_{cJ}$, $\Upsilon$, $\chi_{bJ}$ at the LHC. We find that the associated production of prompt $\mathcal{Q} = J/\psi$, $\chi_{cJ}$, $\Upsilon$, $\chi_{bJ}$ and a massive (anti)bottom quark at the LHC have the potential to be detected. When $p_T$ is smaller than about 10 GeV, the $c\bar{c}[^1S_0^{(8)}]$ state give the main contribution to the $p_T$ distribution of prompt $J/\psi$ with a massive (anti)bottom quark production. For the process $pp \to \Upsilon + b(\bar{b})$, the contribution of the CSM is larger than that in the COM at low $p_T$ region. We also investigate the processes of $pp \to \chi_{cJ} + b(\bar{b})$ and $pp \to \chi_{bJ} + b(\bar{b})$, the $p_T$ distribution are dominated by the CO Fock-state contribution at the large $p_T$ region. These processes provide an interesting signature that could be studied at the LHC, and the measurement of these processes is useful to test the CSM and COM.

## ACKNOWLEDGMENTS

This work was supported in part by the Key Research Foundation of Education Ministry of Anhui Province of China (No. KJ2012A021), the Youth Foundation of Anhui University, and financed by the 211 Project of Anhui University.

## APPENDIX

In this Appendix, we list the differential cross sections $d\hat{\sigma}/d\hat{t}$ for processes ${}_g b \to QQ[n] + b$. Our results read

$$\frac{d\sigma}{d\hat{t}}(gb \to c\bar{c}[^1S_0^{(1)}]b) = \frac{4\alpha_s^3\pi^2}{9m_c\hat{t}^2(-4m_c^2+\hat{t})^2\hat{s}^2}[2m_b^4(8m_c^2-\hat{t}) - 16m_c^4(\hat{s}+\hat{u}) + 4m_c^2(\hat{s}+\hat{u})(\hat{s}+\hat{t}+\hat{u}) - \hat{t}(\hat{s}^2+\hat{u}^2) - 2m_b^2(\hat{t}(-\hat{s}+\hat{t}-\hat{u}) + m_c^2(8\hat{s}-4\hat{t}+8\hat{u}))],$$

$$\frac{d\sigma}{d\hat{t}}(gb \to c\bar{c}[^1S_0^{(8)}]b) = \frac{5\alpha_s^3\pi^2}{36m_c\hat{t}^2(-4m_c^2+\hat{t})^2\hat{s}^2}[2m_b^4(8m_c^2-\hat{t}) - 16m_c^4(\hat{s}+\hat{u}) + 4m_c^2(\hat{s}+\hat{u})(\hat{s}+\hat{t}+\hat{u}) - \hat{t}(\hat{s}^2+\hat{u}^2) - 2m_b^2(\hat{t}(-\hat{s}+\hat{t}-\hat{u}) + m_c^2(8\hat{s}-4\hat{t}+8\hat{u}))],$$

$$\frac{d\sigma}{d\hat{t}}(gb \to c\bar{c}[^3S_1^{(1)}]b) = 0,$$

$$\frac{d\sigma}{d\hat{t}}(gb \to c\bar{c}[^3S_1^{(8)}]b) = \frac{\alpha_s^3\pi^2(7m_b^4+4\hat{s}^2-\hat{s}\,\hat{u}+4\hat{u}^2-7m_b^2(\hat{s}+\hat{u}))}{216m_c^3(m_b^2-\hat{s})^2(m_b^2-\hat{u})^2(-2m_b^2+\hat{s}+\hat{u})^2\hat{s}^2}[6m_b^8 - \hat{s}\,\hat{u}(32m_c^4+\hat{s}^2+\hat{u}^2-8m_c^2(\hat{s}+\hat{u})) - m_b^4(32m_c^4+3\hat{s}^2+14\hat{s}\,\hat{u}+3\hat{u}^2-8m_c^2(\hat{s}+\hat{u})) + m_b^2(\hat{s}^3-32m_c^2\hat{s}\,\hat{u}+7\hat{s}^2\hat{u}+7\hat{s}\hat{u}^2+\hat{u}^3 + 32m_c^4(\hat{s}+\hat{u}))],$$

$$\frac{d\sigma}{d\hat{t}}(gb \to c\bar{c}[^1P_1^{(1)}]b) = 0,$$

$$\frac{d\sigma}{d\hat{t}}(gb \to c\bar{c}[^1P_1^{(8)}]b) = \frac{-\alpha_s^3\pi^2}{12m_c^3\hat{t}^2(-4m_c^2+\hat{t})^2\hat{s}^2}[2m_b^4\hat{t}+4m_b^2(8m_c^4-2m_c^2\hat{t}-\hat{s}\,\hat{t})+\hat{t}(16m_c^4+2\hat{s}^2+2\hat{s}\,\hat{t}+\hat{t}^2-8m_c^2(\hat{s}+\hat{t}))],$$

$$\frac{d\sigma}{d\hat{t}}(gb \to c\bar{c}[^3P_J^{(1)}]b) = \frac{4\alpha_s^3\pi^2}{9\hat{t}^2(-4m_c^3+m_c\hat{t})^3\hat{s}^2}[2m_b^4(28m_c^2-3\hat{t})\hat{t}+4m_b^2(224m_c^6-16m_c^4\hat{t}+3s\hat{t}^2-2m_c^2\hat{t}(14\hat{s}+5\hat{t})) + \hat{t}(448m_c^6-16m_c^4(14\hat{s}+9\hat{t})-3\hat{t}(2\hat{s}^2+2\hat{s}\,\hat{t}+\hat{t}^2)+4m_c^2(14\hat{s}^2+20\hat{s}\,\hat{t}+5\hat{t}^2))],$$

$$\frac{d\sigma}{d\hat{t}}(gb \to c\bar{c}[^3P_J^{(8)}]b) = \frac{5\alpha_s^3\pi^2}{36\hat{t}^2(-4m_c^3+m_c\hat{t})^3\hat{s}^2}[2m_b^4(28m_c^2-3\hat{t})\hat{t}+4m_b^2(224m_c^6-16m_c^4\hat{t}+3\hat{s}\hat{t}^2-2m_c^2\hat{t}(14\hat{s}+5\hat{t})) + \hat{t}(448m_c^6-16m_c^4(14\hat{s}+9\hat{t})-3\hat{t}(2\hat{s}^2+2\hat{s}\,\hat{t}+\hat{t}^2)+4m_c^2(14\hat{s}^2+20\hat{s}\,\hat{t}+5\hat{t}^2))],$$

$$\frac{d\sigma}{d\hat{t}}(gb \to b\bar{b}[^1S_0^{(1)}]b) = \frac{-4\alpha_s^3\pi^2}{81m_b(m_b^2-\hat{s})^4\hat{t}^2(-4m_b^2+\hat{t})^2(-5m_b^2+\hat{s}+\hat{t})^4\hat{s}^2}[180000m_b^{22} - 150m_b^{20}(5760\hat{s}-9527\hat{t}) + 4m_b^{18}(424800\hat{s}^2-915255\hat{s}\,\hat{t}-908548\hat{t}^2)+\hat{s}^2\hat{t}(2\hat{s}^2+2\hat{s}\,\hat{t}+\hat{t}^2)(-3\hat{s}^3-6\hat{s}^2\hat{t}+\hat{s}\hat{t}^2+4\hat{t}^3)^2 + m_b^{16}(-1762560\hat{s}^3+3317322\hat{s}^2\hat{t}+4092858\hat{s}\hat{t}^2+3266069\hat{t}^3)+4m_b^{14}(259632\hat{s}^4-394884\hat{s}^3\hat{t} - 863500\hat{s}^2\hat{t}^2-327052\hat{s}\hat{t}^3-374113\hat{t}^4)-4m_b^{12}(88128\hat{s}^5-206589\hat{s}^4\hat{t}-287598\hat{s}^3\hat{t}^2 - 325069\hat{s}^2\hat{t}^3+18200\hat{s}\hat{t}^4-98252\hat{t}^5)+4m_b^{10}(16992\hat{s}^6-122202\hat{s}^5\hat{t}-106508\hat{s}^4\hat{t}^2+3416\hat{s}^3\hat{t}^3 - 95855\hat{s}^2\hat{t}^4+34362\hat{s}\hat{t}^5-15623\hat{t}^6)+m_b^8(-6912\hat{s}^7+198756\hat{s}^6\hat{t}+253116\hat{s}^5\hat{t}^2-143898\hat{s}^4\hat{t}^3 - 90600\hat{s}^3\hat{t}^4+132856\hat{s}^2\hat{t}^5-28370\hat{s}\hat{t}^6+6313\hat{t}^7)+4m_b^6(72\hat{s}^8-12132\hat{s}^7\hat{t}-24340\hat{s}^6\hat{t}^2 + 2724\hat{s}^5\hat{t}^3+23713\hat{s}^4\hat{t}^4+1300\hat{s}^3\hat{t}^5-9188\hat{s}^2\hat{t}^6+177\hat{s}\hat{t}^7-106\hat{t}^8)-4m_b^2\hat{s}\,\hat{t}(135\hat{s}^8+528\hat{s}^7\hat{t} + 528\hat{s}^6\hat{t}^2-271\hat{s}^5\hat{t}^3-690\hat{s}^4\hat{t}^4-215\hat{s}^3\hat{t}^5+187\hat{s}^2\hat{t}^6+126\hat{s}\hat{t}^7+8\hat{t}^8)+2m_b^4\hat{t}(3465\hat{s}^8 + 10044\hat{s}^7\hat{t}+4450\hat{s}^6\hat{t}^2-9384\hat{s}^5\hat{t}^3-7888\hat{s}^4\hat{t}^4+1994\hat{s}^3\hat{t}^5+3007\hat{s}^2\hat{t}^6+188\hat{s}\hat{t}^7+8\hat{t}^8)],$$

$$\frac{d\sigma}{d\hat{t}}(gb \to b\bar{b}[^1S_0^{(8)}]b) = \frac{-\alpha_s^3\pi^2}{324m_b(m_b^2-\hat{s})^4\hat{t}^2(-4m_b^2+\hat{t})^2(-5m_b^2+\hat{s}+\hat{t})^4\hat{s}^2}[900000m_b^{22} - 750m_b^{20}(5760\hat{s}+2569\hat{t}) + 4m_b^{18}(2124000\hat{s}^2+1514925\hat{s}\,\hat{t}-292642\hat{t}^2) + m_b^{16}(-8812800\hat{s}^3-6758670\hat{s}^2\hat{t} + 3117666\hat{s}\hat{t}^2+1530353\hat{t}^3) + 8m_b^{14}(649080\hat{s}^4+282870\hat{s}^3\hat{t}-797714\hat{s}^2\hat{t}^2 - 401132\hat{s}\hat{t}^3-72893\hat{t}^4) + 4m_b^{12}(-440640\hat{s}^5+432465\hat{s}^4\hat{t}+1876374\hat{s}^3\hat{t}^2 + 1308895\hat{s}^2\hat{t}^3+231988\hat{s}\hat{t}^4+29447\hat{t}^5) + 4m_b^{10}(84960\hat{s}^6-533250\hat{s}^5\hat{t}-1391312\hat{s}^4\hat{t}^2 - 1158952\hat{s}^3\hat{t}^3-439340\hat{s}^2\hat{t}^4-33147\hat{s}\hat{t}^5-3587\hat{t}^6) + \hat{s}^2\hat{t}(\hat{s}+\hat{t})^2(90\hat{s}^6+270\hat{s}^5\hat{t} + 363\hat{s}^4\hat{t}^2+276\hat{s}^3\hat{t}^3+125\hat{s}^2\hat{t}^4+32\hat{s}\hat{t}^5+4\hat{t}^6) + m_b^8(-34560\hat{s}^7+976500\hat{s}^6\hat{t} + 2600172\hat{s}^5\hat{t}^2+2623254\hat{s}^4\hat{t}^3+1433016\hat{s}^3\hat{t}^4+381832\hat{s}^2\hat{t}^5+9382\hat{s}\hat{t}^6+1141\hat{t}^7) + 4m_b^6(360\hat{s}^8-60660\hat{s}^7\hat{t}-186316\hat{s}^6\hat{t}^2-233112\hat{s}^5\hat{t}^3-165986\hat{s}^4\hat{t}^4-72110\hat{s}^3\hat{t}^5 - 13166\hat{s}^2\hat{t}^6-78\hat{s}\hat{t}^7-19\hat{t}^8) + 2m_b^4\hat{t}(17325\hat{s}^8+63180\hat{s}^7\hat{t}+97678\hat{s}^6\hat{t}^2+87168\hat{s}^5\hat{t}^3 + 50438\hat{s}^4\hat{t}^4+17006\hat{s}^3\hat{t}^5+1993\hat{s}^2t^6+32\hat{s}\hat{t}^7+2\hat{t}^8) - 4m_b^2\hat{s}\,\hat{t}(675\hat{s}^8+2910\hat{s}^7\hat{t} + 5448\hat{s}^6\hat{t}^2+5912\hat{s}^5\hat{t}^3+4167\hat{s}^4\hat{t}^4+1915\hat{s}^3\hat{t}^5+484\hat{s}^2\hat{t}^6+39\hat{s}\hat{t}^7+2\hat{t}^8)],$$

$$\frac{d\sigma}{d\hat{t}}(gb \to b\bar{b}[^3S_1^{(1)}]b) = \frac{-32\alpha_s^3\pi^2}{243m_b(m_b^2-\hat{s})^4(m_b^2-\hat{u})^4(-2m_b^2+\hat{s}+\hat{u})^2\hat{s}^2}[5466m_b^{18} - 18668m_b^{16}(\hat{s}+\hat{u}) - 2\hat{s}^2\hat{u}^2(\hat{s}+\hat{u})^3(9\hat{s}^2+16\hat{s}\,\hat{u}+9\hat{u}^2) + m_b^{14}(23389\hat{s}^2+62070\hat{s}\,\hat{u}+23389\hat{u}^2) - m_b^{12}(14251\hat{s}^3+73585\hat{s}^2\hat{u}+73585\hat{s}\hat{u}^2+14251\hat{u}^3) + m_b^{10}(4609\hat{s}^4+43259\hat{s}^3\hat{u} + 74588\hat{s}^2\hat{u}^2+43259\hat{s}\hat{u}^3+4609\hat{u}^4) - m_b^8(807\hat{s}^5+14717\hat{s}^4\hat{u}+35184\hat{s}^3\hat{u}^2 + 35184\hat{s}^2\hat{u}^3+14717\hat{s}\hat{u}^4+807\hat{u}^5) + m_b^2\hat{s}\,\hat{u}(20\hat{s}^6+228\hat{s}^5\hat{u}+701\hat{s}^4\hat{u}^2+984\hat{s}^3\hat{u}^3 + 701\hat{s}^2\hat{u}^4+228\hat{s}\hat{u}^5+20\hat{u}^6) + m_b^6(72\hat{s}^6+3179\hat{s}^5\hat{u}+9455\hat{s}^4\hat{u}^2+12444\hat{s}^3\hat{u}^3 + 9455\hat{s}^2\hat{u}^4+3179\hat{s}\hat{u}^5+72\hat{u}^6) - m_b^4(2\hat{s}^7+406\hat{s}^6\hat{u}+1753\hat{s}^5\hat{u}^2+3043\hat{s}^4\hat{u}^3 + 3043\hat{s}^3\hat{u}^4+1753\hat{s}^2\hat{u}^5+406\hat{s}\hat{u}^6+2\hat{u}^7)],$$

$$\frac{d\sigma}{d\hat{t}}(gb \to b\bar{b}[^3S_1^{(8)}]b) = \frac{-\alpha_s^3\pi^2}{1944m_b^3(m_b^2-s)^4(m_b^2-\hat{u})^4(-2m_b^2+\hat{s}+\hat{u})^2\hat{s}^2}[66174m_b^{20} - 226934m_b^{18}(\hat{s}+\hat{u}) + m_b^{16}(260287\hat{s}^2+806952\hat{s}\,\hat{u}+260287\hat{u}^2) - 10m_b^{14}(10975\hat{s}^3+96181\hat{s}^2\hat{u}+96181\hat{s}\hat{u}^2 + 10975\hat{u}^3) + 9\hat{s}^3\hat{u}^3(4\hat{s}^4-\hat{s}^3\hat{u}+8\hat{s}^2\hat{u}^2-\hat{s}\hat{u}^3+4\hat{u}^4) + 2m_b^{12}(6155\hat{s}^4+216310\hat{s}^3\hat{u} + 584812\hat{s}^2\hat{u}^2+216310\hat{s}\hat{u}^3+6155\hat{u}^4) - 2m_b^2\hat{s}^2\hat{u}^2(90\hat{s}^5+493\hat{s}^4\hat{u}+468\hat{s}^3\hat{u}^2 + 468\hat{s}^2\hat{u}^3+493\hat{s}\hat{u}^4+90\hat{u}^5) - 2m_b^{10}(1548\hat{s}^5+27601\hat{s}^4\hat{u}+266181\hat{s}^3\hat{u}^2 + 266181\hat{s}^2\hat{u}^3+27601\hat{s}\hat{u}^4+1548\hat{u}^5) + 2m_b^4\hat{s}\,\hat{u}(94\hat{s}^6+534\hat{s}^5\hat{u}+3748\hat{s}^4\hat{u}^2 - 477\hat{s}^3\hat{u}^3+3748\hat{s}^2\hat{u}^4+534\hat{s}\hat{u}^5+94\hat{u}^6) + m_b^8(285\hat{s}^6+9920\hat{s}^5\hat{u}+60701\hat{s}^4\hat{u}^2 + 245736\hat{s}^3\hat{u}^3+60701\hat{s}^2\hat{u}^4+9920\hat{s}\hat{u}^5+285\hat{u}^6) - 2m_b^6(22\hat{s}^7+563\hat{s}^6\hat{u}+4424\hat{s}^5\hat{u}^2 + 13715\hat{s}^4\hat{u}^3+13715\hat{s}^3\hat{u}^4+4424\hat{s}^2\hat{u}^5+563\hat{s}\hat{u}^6+22\hat{u}^7)],$$

$$\frac{d\sigma}{d\hat{t}}(gb \to b\bar{b}[^1P_1^{(1)}]b) = \frac{64\alpha_s^3\pi^2}{243(m_b^2-\hat{s})^5(-5m_b^2+\hat{s}+\hat{t})^5(4m_b^3-m_b\hat{t})^3\hat{s}^2}[2227744m_b^{24} - 2m_b^{22}(10071936\hat{s} + 1099435\hat{t})$$
$$- \hat{s}^3\hat{t}^4(\hat{s}+\hat{t})^3(2\hat{s}^2 + 2\hat{s}\,\hat{t} + 9\hat{t}^2) + m_b^{20}(-6754944\hat{s}^2 + 28431108\hat{s}\,\hat{t} + 367984\hat{t}^2)$$
$$+ m_b^{18}(12743424\hat{s}^3 + 25261690\hat{s}^2\hat{t} - 16277654\hat{s}\hat{t}^2 + 488169\hat{t}^3) - 2m_b^{16}(3126432\hat{s}^4$$
$$+ 13119432\hat{s}^3\hat{t} + 14986264\hat{s}^2\hat{t}^2 - 2170280\hat{s}\hat{t}^3 + 183541\hat{t}^4) + 4m_b^{14}(409536\hat{s}^5$$
$$+ 2567733\hat{s}^4\hat{t} + 5640894\hat{s}^3\hat{t}^2 + 4564301\hat{s}^2\hat{t}^3 - 49258\hat{s}\hat{t}^4 + 32054\hat{t}^5)$$
$$+ m_b^2\hat{s}^2\hat{t}(\hat{s}+\hat{t})^2(2\hat{s}^6 + 6\hat{s}^5\hat{t} + 35\hat{s}^4\hat{t}^2 + 108\hat{s}^3\hat{t}^3 + 249\hat{s}^2\hat{t}^4 + 334\hat{s}\hat{t}^5 + 27\hat{t}^6)$$
$$- m_b^{12}(257664\hat{s}^6 + 2250792\hat{s}^5\hat{t} + 7210544\hat{s}^4\hat{t}^2 + 10902208\hat{s}^3\hat{t}^3 + 6680880\hat{s}^2\hat{t}^4$$
$$+ 222148\hat{s}\hat{t}^5 + 27053\hat{t}^6) + 2m_b^{10}(11904\hat{s}^7 + 152098\hat{s}^6\hat{t} + 651630\hat{s}^5\hat{t}^2 + 1443207\hat{s}^4\hat{t}^3$$
$$+ 1656100\hat{s}^3\hat{t}^4 + 780410\hat{s}^2\hat{t}^5 + 36206\hat{s}\hat{t}^6 + 1776\hat{t}^7) + m_b^6\hat{t}(1474\hat{s}^8 + 10168\hat{s}^7\hat{t}$$
$$+ 36644\hat{s}^6\hat{t}^2 + 87208\hat{s}^5\hat{t}^3 + 125184\hat{s}^4\hat{t}^4 + 88392\hat{s}^3\hat{t}^5 + 22168\hat{s}^2\hat{t}^6 + 836\hat{s}\hat{t}^7 + 9\hat{t}^8)$$
$$- m_b^4\hat{s}\,\hat{t}(60\hat{s}^8 + 448\hat{s}^7\hat{t} + 1888\hat{s}^6\hat{t}^2 + 5568\hat{s}^5\hat{t}^3 + 11620\hat{s}^4\hat{t}^4 + 14011\hat{s}^3\hat{t}^5$$
$$+ 7614\hat{s}^2\hat{t}^6 + 1182\hat{s}\hat{t}^7 + 27\hat{t}^8) - m_b^8(992\hat{s}^8 + 26384\hat{s}^7\hat{t} + 143952\hat{s}^6\hat{t}^2 + 424880\hat{s}^5\hat{t}^3$$
$$+ 736548\hat{s}^4\hat{t}^4 + 663440\hat{s}^3\hat{t}^5 + 235347\hat{s}^2\hat{t}^6 + 10823\hat{s}\hat{t}^7 + 269\hat{t}^8)],$$

$$\frac{d\sigma}{d\hat{t}}(gb \to b\bar{b}[^3P_J^{(1)}]b) = \frac{4\alpha_s^3\pi^2}{81(m_b^2-\hat{s})^5\hat{t}^2(-5m_b^2+\hat{s}+\hat{t})^5(4m_b^3-m_b\hat{t})^3\hat{s}^2}[25200000m_b^{28} - 600m_b^{26}(252000\hat{s}$$
$$+ 346111\hat{t}) - 3\hat{s}^3\hat{t}^2(\hat{s}+\hat{t})^3(3\hat{s}^2 + 3\hat{s}\,\hat{t} - 4\hat{t}^2)^2(2\hat{s}^2 + 2\hat{s}\,\hat{t} + \hat{t}^2) + 18m_b^{24}(21560000\hat{s}^2$$
$$+ 26837680\hat{s}\,\hat{t} + 6879209\hat{t}^2) - 6m_b^{22}(92736000\hat{s}^3 + 58438984\hat{s}^2\hat{t} + 132101836\hat{s}\hat{t}^2$$
$$- 31650279\hat{t}^3) + m_b^{20}(489081600\hat{s}^4 + 52223904\hat{s}^3\hat{t} - 596240052\hat{s}^2\hat{t}^2 + 475090104\hat{s}\hat{t}^3$$
$$- 316136919\hat{t}^4) + 3m_b^{18}(-91058688\hat{s}^5 + 34245912\hat{s}^4\hat{t} + 252722648\hat{s}^3\hat{t}^2$$
$$+ 543856590\hat{s}^2\hat{t}^3 + 29438668\hat{s}\hat{t}^4 + 71917105\hat{t}^5) + m_b^{16}(97816320\hat{s}^6 - 160017984\hat{s}^5\hat{t}$$
$$- 491228090\hat{s}^4\hat{t}^2 - 877626916\hat{s}^3\hat{t}^3 - 1687844825\hat{s}^2\hat{t}^4 - 268763655\hat{s}\hat{t}^5 - 87840460\hat{t}^6)$$
$$+ 4m_b^{14}(-5564160\hat{s}^7 + 30448824\hat{s}^6\hat{t} + 75718764\hat{s}^5\hat{t}^2 + 66864981\hat{s}^4\hat{t}^3$$
$$+ 140914224\hat{s}^3\hat{t}^4 + 246581099\hat{s}^2\hat{t}^5 + 40404191\hat{s}\hat{t}^6 + 5840348\hat{t}^7) + m_b^{12}(3104640\hat{s}^8$$
$$- 54127296\hat{s}^7\hat{t} - 151809336\hat{s}^6\hat{t}^2 - 114986592\hat{s}^5\hat{t}^3 - 65176694\hat{s}^4\hat{t}^4 - 23885172\hat{s}^3\hat{t}^5$$
$$- 3599851\hat{s}^2\hat{t}^6 - 522139\hat{s}\hat{t}^7 - 41310\hat{t}^8) + m_b^2\hat{s}^2\hat{t}(\hat{s}+\hat{t})^2(504\hat{s}^8 + 3960\hat{s}^7\hat{t}$$
$$+ 8522\hat{s}^6\hat{t}^2 + 3336\hat{s}^5\hat{t}^3 - 4911\hat{s}^4\hat{t}^4 - 1942\hat{s}^3\hat{t}^5 + 791\hat{s}^2\hat{t}^6 + 416\hat{s}\hat{t}^7 + 1552\hat{t}^8)$$
$$+ m_b^{10}(-241920\hat{s}^9 + 14973288\hat{s}^8\hat{t} + 51568272\hat{s}^7\hat{t}^2 + 52527524\hat{s}^6\hat{t}^3 + 13171944\hat{s}^5\hat{t}^4$$
$$+ 8800346\hat{s}^4\hat{t}^5 + 67284444\hat{s}^3\hat{t}^6 + 85100380\hat{s}^2\hat{t}^7 + 10250336\hat{s}\hat{t}^8 + 471419\hat{t}^9)$$
$$+ m_b^8(8064\hat{s}^{10} - 2633760\hat{s}^9\hat{t} - 11282354\hat{s}^8\hat{t}^2 - 15962360\hat{s}^7\hat{t}^3 - 7053666\hat{s}^6\hat{t}^4$$
$$+ 1332094\hat{s}^5\hat{t}^5 - 874708\hat{s}^4\hat{t}^6 - 12363406\hat{s}^3\hat{t}^7 - 13033959\hat{s}^2\hat{t}^8 - 1228903\hat{s}\hat{t}^9$$
$$- 31560\hat{t}^{10}) + 2m_b^6\hat{t}(144360\hat{s}^{10} + 773580\hat{s}^9\hat{t} + 1467393\hat{s}^8\hat{t}^2 + 1038192\hat{s}^7\hat{t}^3$$
$$+ 56862\hat{s}^6\hat{t}^4 - 231222\hat{s}^5\hat{t}^5 + 62812\hat{s}^4\hat{t}^6 + 716948\hat{s}^3\hat{t}^7 + 623079\hat{s}^2\hat{t}^8 + 41600\hat{s}\hat{t}^9$$
$$+ 472\hat{t}^{10}) - m_b^4\hat{s}\,\hat{t}(18144\hat{s}^{10} + 124628\hat{s}^9\hat{t} + 311800\hat{s}^8\hat{t}^2 + 318915\hat{s}^7\hat{t}^3 + 73212\hat{s}^6\hat{t}^4$$
$$- 68716\hat{s}^5\hat{t}^5 - 37362\hat{s}^4\hat{t}^6 + 24645\hat{s}^3\hat{t}^7 + 98510\hat{s}^2\hat{t}^8 + 67280\hat{s}\hat{t}^9 + 2448\hat{t}^{10})],$$

$$\frac{d\sigma}{d\hat{t}}(gb \to b\bar{b}[^3P_J^{(8)}]b) = \frac{\alpha_s^3\pi^2}{324(m_b^2-\hat{s})^5\hat{t}^2(-5m_b^2+\hat{s}+\hat{t})^5(4m_b^3-m_b\hat{t})^3\hat{s}^2}[126000000m_b^{28} - 21000m_b^{26}(36000\hat{s} - 5111\hat{t}) + 6m_b^{24}(323400000\hat{s}^2 - 107724005\hat{s}\,\hat{t} - 179385097\hat{t}^2) - 6m_b^{22}(463680000\hat{s}^3 + 66541160\hat{s}^2\hat{t} - 356589988\hat{s}\hat{t}^2 - 199413487\hat{t}^3) + 3m_b^{20}(815136000\hat{s}^4 + 161689440\hat{s}^3\hat{t} - 713740812\hat{s}^2\hat{t}^2 - 765731304\hat{s}\hat{t}^3 - 210248369\hat{t}^4) - 3m_b^{18}(455293440\hat{s}^5 - 60499320\hat{s}^4\hat{t} - 839359544\hat{s}^3\hat{t}^2 - 998696926\hat{s}^2\hat{t}^3 - 412742996\hat{s}\hat{t}^4 - 69091505\hat{t}^5) + m_b^{16}(489081600\hat{s}^6 - 695580480\hat{s}^5\hat{t} - 3191554274\hat{s}^4\hat{t}^2 - 3864588148\hat{s}^3\hat{t}^3 - 2108766941\hat{s}^2\hat{t}^4 - 451377411\hat{s}\hat{t}^5 - 49514524\hat{t}^6) - 3\hat{s}^3\hat{t}^2(\hat{s}+\hat{t})^3(90\hat{s}^6 + 270\hat{s}^5\hat{t} + 363\hat{s}^4\hat{t}^2 + 276\hat{s}^3\hat{t}^3 + 125\hat{s}^2\hat{t}^4 + 32\hat{s}\hat{t}^5 + 4\hat{t}^6) + 4m_b^{14}(-27820800\hat{s}^7 + 147889560\hat{s}^6\hat{t} + 590044860\hat{s}^5\hat{t}^2 + 991176813\hat{s}^4\hat{t}^3 + 673013160\hat{s}^3\hat{t}^4 + 228128459\hat{s}^2\hat{t}^5 + 31137503\hat{s}\hat{t}^6 + 2314418\hat{t}^7) + m_b^{12}(15523200\hat{s}^8 - 268977600\hat{s}^7\hat{t} - 1077142104\hat{s}^6\hat{t}^2 - 2165379264\hat{s}^5\hat{t}^3 - 2341866062\hat{s}^4\hat{t}^4 - 1031915260\hat{s}^3\hat{t}^5 - 254801556\hat{s}^2\hat{t}^6 - 25728466\hat{s}\hat{t}^7 - 1320599\hat{t}^8) + m_b^2\hat{s}^2\hat{t}(\hat{s}+\hat{t})^2(2520\hat{s}^8 + 19800\hat{s}^7\hat{t} + 51098\hat{s}^6\hat{t}^2 + 68064\hat{s}^5\hat{t}^3 + 64785\hat{s}^4\hat{t}^4 + 48194\hat{s}^3\hat{t}^5 + 17783\hat{s}^2\hat{t}^6 + 344\hat{s}\hat{t}^7 + 388\hat{t}^8) + m_b^{10}(-1209600\hat{s}^9 + 74797320\hat{s}^8\hat{t} + 324287952\hat{s}^7\hat{t}^2 + 702527876\hat{s}^6\hat{t}^3 + 1006700472\hat{s}^5\hat{t}^4 + 755209754\hat{s}^4\hat{t}^5 + 232438668\hat{s}^3\hat{t}^6 + 46247836\hat{s}^2\hat{t}^7 + 3738896\hat{s}\hat{t}^8 + 131591\hat{t}^9) + m_b^8(40320\hat{s}^{10} - 13168800\hat{s}^9\hat{t} - 64937498\hat{s}^8\hat{t}^2 - 149484440\hat{s}^7\hat{t}^3 - 240269802\hat{s}^6\hat{t}^4 - 255755594\hat{s}^5\hat{t}^5 - 139606876\hat{s}^4\hat{t}^6 - 30968470\hat{s}^3\hat{t}^7 - 5385543\hat{s}^2\hat{t}^8 - 359983\hat{s}\hat{t}^9 - 8100\hat{t}^{10}) + 2m_b^6\hat{t}(721800\hat{s}^{10} + 4187100\hat{s}^9\hat{t} + 10660281\hat{s}^8\hat{t}^2 + 17776032\hat{s}^7\hat{t}^3 + 22160286\hat{s}^6\hat{t}^4 + 17930202\hat{s}^5\hat{t}^5 + 7326376\hat{s}^4\hat{t}^6 + 1157204\hat{s}^3\hat{t}^7 + 196287\hat{s}^2\hat{t}^8 + 10640\hat{s}\hat{t}^9 + 118\hat{t}^{10}) - m_b^4\hat{s}\,\hat{t}(90720\hat{s}^{10} + 644420\hat{s}^9\hat{t} + 1920040\hat{s}^8\hat{t}^2 + 3393519\hat{s}^7\hat{t}^3 + 4354860\hat{s}^6\hat{t}^4 + 4215260\hat{s}^5\hat{t}^5 + 2625438\hat{s}^4\hat{t}^6 + 805269\hat{s}^3\hat{t}^7 + 84038\hat{s}^2\hat{t}^8 + 17240\hat{s}\hat{t}^9 + 612\hat{t}^{10})].$$


[1] M. B. Einhorn and S. D. Ellis, Phys. Rev. D **12**, 2007 (1975); S. D. Ellis, M. B. Einhorn, and C. Quigg, Phys. Rev. Lett. **36**, 1263 (1976); Chang Chao-Hsi, Nucl. Phys. **B172**, 425 (1980); E. L. Berger and D. L. Jones, Phys. Rev. D **23**, 1521 (1981); R. Baier and R. Ruckl, Nucl. Phys. **B201**, 1 (1982).

[2] R. Barbieri, R. Gatto, and E. Remiddi, Phys. Lett. B **61**, 465 (1976); R. Barbieri, M. Caffo, R. Gatto, and E. Remiddi, Phys. Lett. B **95**, 93 (1980); Nucl. Phys. **B192**, 61 (1981); R. Barbieri, E. d'Emilio, G. Curci, and E. Remiddi, Nucl. Phys. **B154**, 535 (1979); K. Hagiwara, C. B. Kim, and T. Yoshino, Nucl. Phys. **B177**, 461 (1981); P. B. Mackenzie and G. P. Lepage, Phys. Rev. Lett. **47**, 1244 (1981).

[3] F. Abe *et al.* (CDF), Phys. Rev. Lett. **69**, 3704 (1992); **71**, 2537 (1993).

[4] G. T. Bodwin, E. Braaten, and G. P. Lepage, Phys. Rev. D **51**, 1125 (1995); **55**, 5853(E) (1997).

[5] G. P. Lepage, L. Magnea, C. Nakhleh, U. Magnea, and K. Hornbostel, Phys. Rev. D **46**, 4052 (1992).

[6] Peter Cho and Adam K. Leibovich, Phys. Rev. D **53**, 150 (1996).

[7] Han-Wen Huang and Kuang-Ta Chao, Phys. Rev. D **54**, 3065 (1996); **55**, 244 (1997); **54**, 6850 (1996).

[8] A. Petrelli, M. Cacciari, M. Greco, F. Maltoni, and M. L. Mangano, Nucl. Phys. **B514**, 245 (1998).

[9] Zhi-Guo He, Ying Fan, and Kuang-Ta Chao, Phys. Rev. Lett. **101**, 112001 (2008).

[10] Ying Fan, Zhi-Guo He, Yan-Qing Ma, and Kuang-Ta Chao, Phys. Rev. D **80**, 014001 (2009).

[11] E. Braaten and S. Fleming, Phys. Rev. Lett. **74**, 3327 (1995).

[12] J. Abdallah *et al.* (DELPHI Collaboration), Phys. Lett. B **565**, 76 (2003); M. Klasen, B. A. Kniehl, L. N. Mihaila, and M. Steinhauser, Phys. Rev. Lett. **89**, 032001 (2002).

[13] C. Adloff *et al.* (H1 Collaboration), Eur. Phys. J. C **25**, 25 (2002); M. Steder (on behalf of the H1 Collaboration), Report No. H1prelim-07-172.

[14] Mathias Butenschon and Bernd A. Kniehl, Phys. Rev. Lett. **104**, 072001 (2010).

[15] Y. J. Zhang, Y. j. Gao, and K. T. Chao, Phys. Rev. Lett. **96**, 092001 (2006); Y. J. Zhang and K. T. Chao, Phys. Rev. Lett. **98**, 092003 (2007); Y. J. Zhang, Y. Q. Ma, and K. T. Chao, Phys. Rev. D **78**, 054006 (2008); Y. Q. Ma, Y. J.

Zhang, and K. T. Chao, Phys. Rev. Lett. **102**, 162002 (2009); Y. J. Zhang, Y. Q. Ma, K. Wang, and K. T. Chao, Phys. Rev. D **81**, 034015 (2010).

[16] B. Gong and J. X. Wang, Phys. Rev. D **77**, 054028 (2008); Phys. Rev. Lett. **100**, 181803 (2008); **102**, 162003 (2009); Phys. Rev. D **80**, 054015 (2009).

[17] W. L. Sang and Y. Q. Chen, Phys. Rev. D **81**, 034028 (2010).

[18] G. T. Bodwin, D. Kang, T. Kim, J. Lee, and C. Yu, AIP Conf. Proc. **892**, 315 (2007); Z. G. He, Y. Fan, and K. T. Chao, Phys. Rev. D **75**, 074011 (2007); G. T. Bodwin, J. Lee, and C. Yu, Phys. Rev. D **77**, 094018 (2008); Y. Jia, Phys. Rev. D **82**, 034017 (2010).

[19] Z. G. He, Y. Fan, and K. T. Chao, Phys. Rev. D **81**, 054036 (2010).

[20] E. Braaten, B. A. Kniehl, and J. Lee, Phys. Rev. D **62**, 094005 (2000); B. A. Kniehl and J. Lee, Phys. Rev. D **62**, 114027 (2000).

[21] P. Artoisenet, J. Campbell, F. Maltoni, and F. Tramontano, Phys. Rev. Lett. **102**, 142001 (2009); Mathias Butenschoen and Bernd A. Kniehl, Phys. Rev. Lett. **107**, 232001 (2011).

[22] J. P. Lansberg, Phys. Lett. B **679**, 340 (2009); C. H. Kom, A. Kulesza, and W. J. Stirling, Phys. Rev. Lett. **107**, 082002 (2011); Bernd A. Kniehl, Caesar P. Palisoc, and Lennart Zwirner, Phys. Rev. D **66**, 114002 (2002); **69**, 115005 (2004); Rong Li, Yu-Jie Zhang, and Kuang-Ta Chao, Phys. Rev. D **80**, 014020 (2009).

[23] P. Artoisenet, J. P. Lansberg, and F. Maltoni, Phys. Lett. B **653**, 60 (2007).

[24] R. Li and J. X. Wang, Phys. Lett. B **672**, 51 (2009); P. Artoisenet, J. Campbell, J. P. Lansberg, F. Maltoni, and F. Tramontano, Phys. Rev. Lett. **101**, 152001 (2008); Zhi-Guo He, Rong Li, and Jian-Xiong Wang, Phys. Rev. D **79**, 094003 (2009); Bin Gong, Jian-Xiong Wang, and Hong-Fei Zhang, Phys. Rev. D **83**, 114021 (2011).

[25] Li Gang, Song Mao, Zhang Ren-You, and Ma Wen-Gan, Phys. Rev. D **83**, 014001 (2011).

[26] Song Mao, Ma Wen-Gan, Li Gang, Zhang Ren-You, and Guo Lei, J. High Energy Phys. 02 (2011) 071.

[27] V. Barger, S. Fleming, and R. J. N. Phillips, Phys. Lett. B **371**, 111 (1996).

[28] E. Braaten, J. Lee, and S. Fleming, Phys. Rev. D **60**, 091501 (1999).

[29] Yan-Qing Ma, Kai Wang, and Kuang-Ta Chao, Phys. Rev. D **83**, 111503 (2011).

[30] M. Butensch, Madrid, and Spain, AIP Conf. Proc. **1343**, 409 (2011).

[31] E. J. Eichten and C. Quigg, Phys. Rev. D **52**, 1726 (1995).

[32] W. Buchmüller and S. H. H. Tye, Phys. Rev. D **24**, 132 (1981); E. J. Eichten and C. Quigg, Phys. Rev. D **52**, 1726 (1995).

[33] T. Affolder *et al.* (CDF), Phys. Rev. Lett. **84**, 2094 (2000).

[34] J. Pumplin, D. R. Stump, J. Huston, H. L. Lai, P. Nadolsky, and W. K. Tung, J. High Energy Phys. 07 (2002) 012.